Electronic Supplementary Material (ESI) for Journal of Materials Chemistry A.

Improve the Intrinsic Conductivity of δ-MnO_2 by Indium Doping for High Performance Neutral Aqueous Sodium-Ion Supercapacitors with Commercial-Level Mass-Loading

Borui Li[a,b,1], Yanfang Chu [a,1], Bin Xie [a], Yuchen Sun [a], Lin Zhang [a], Hongmei Zhao[c], Lei Zhao[c,*], Peng-Fei Liu[d], Junjie He[a,c,*]

[a]Biomass new materials research center, College of Architectural Engineering, Yunnan Agricultural University, Kunming 650201, China

[b]Department of Chemical and Environmental Engineering, University of Nottingham Ningbo China, Ningbo 315100, China

[c]Yunnan International Joint Research and Development Centre for smart agriculture and water security, Yunnan Agricultural University, Kunming 650201, China

[d]Spallation Neutron Source Science Center, Institute of High Energy Physics, Chinese Academy of Sciences, Dongguan 523803, China

[1]These authors contribute equally to this work.

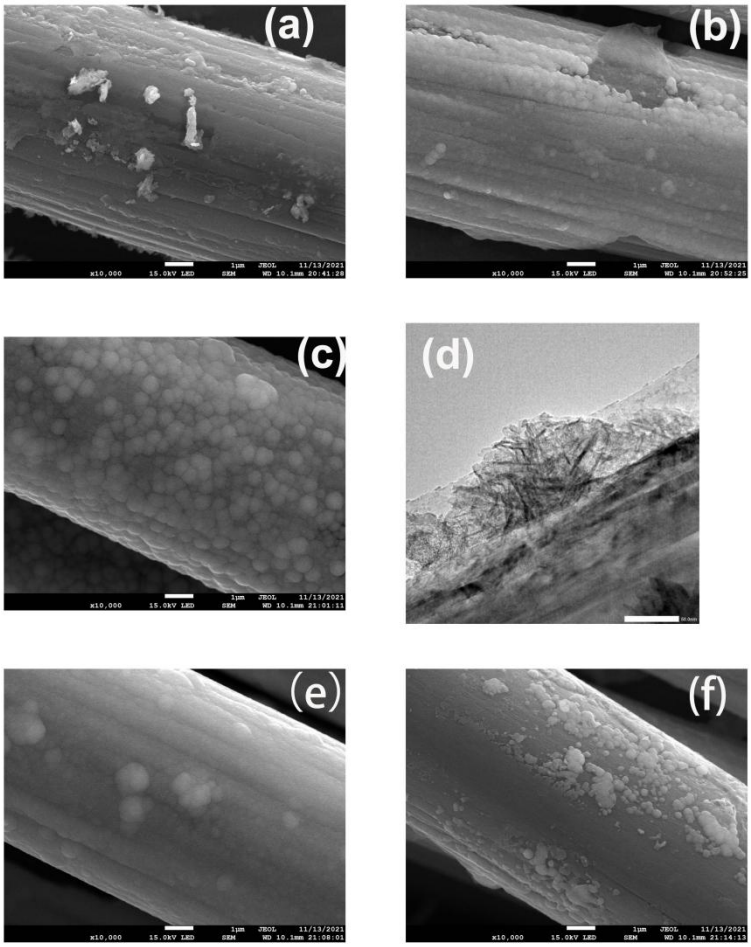

Fig. S 1 (a)~(c) are the SEM images (scale bar: 1 μm) of CC covered by PMO, FeMO and 0.35%InFeMO, respectively. (d) is the TEM image of 0.35%InFeMO. (e) and (f) are the SEM images of CC coverd by 0.7%InFeMO and 1.4%InFeMO (scale bar: 1 μm).

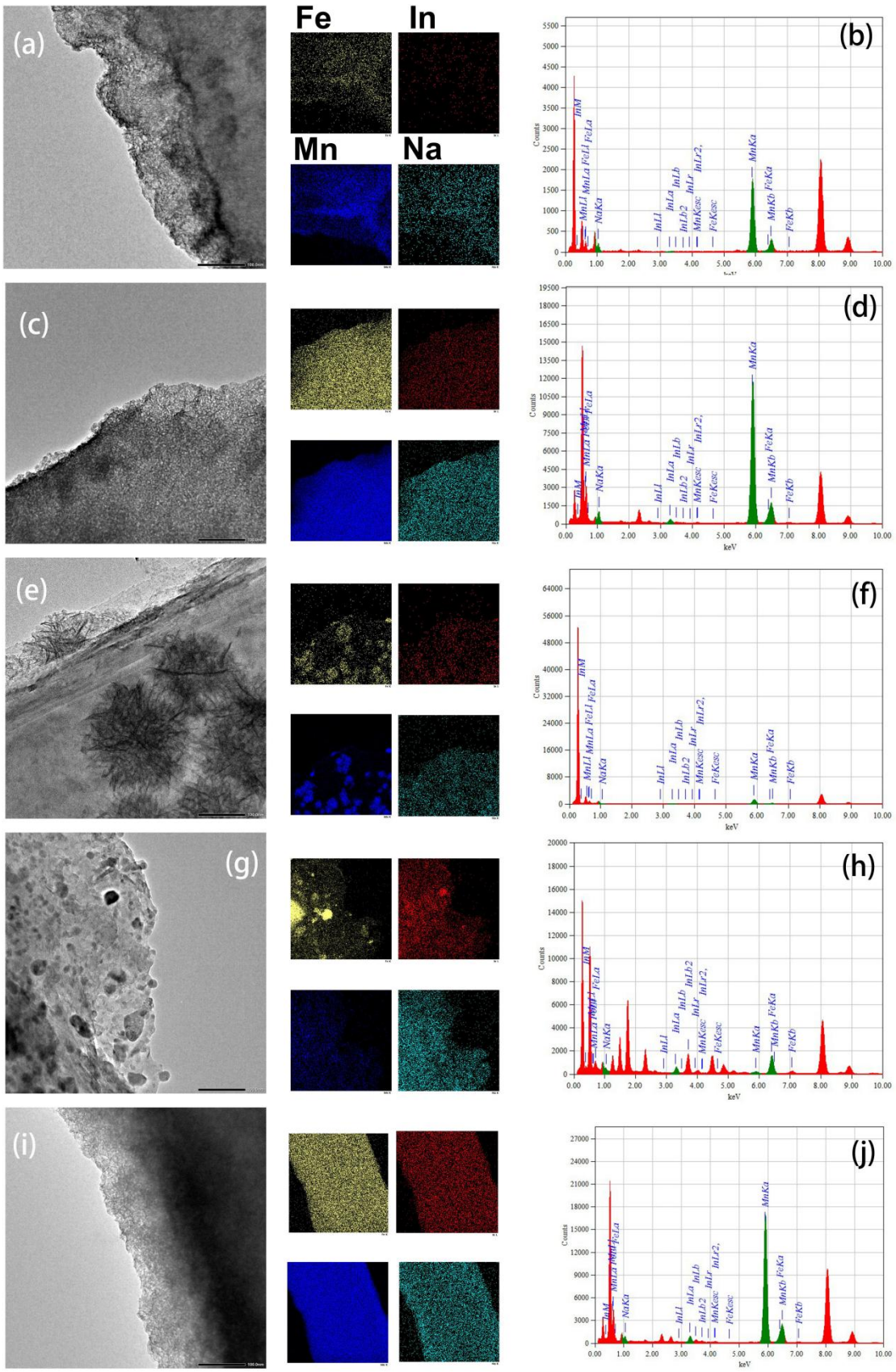

Fig. S 2 TEM images and EDS elemental mapping of the (a) PMO, (c) FeMO, (e) 0.35%InFeMO, (g) 0.7%InFeMO and (i) 1.4%InFeMO. EDS images of the (b) PMO, (d) FeMO, (f) 0.35%InFeMO, (h)

0.7%InFeMO and (j) 1.4%InFeMO. Small amount of Fe in PMO is from the raw material manganese acetate (99%).

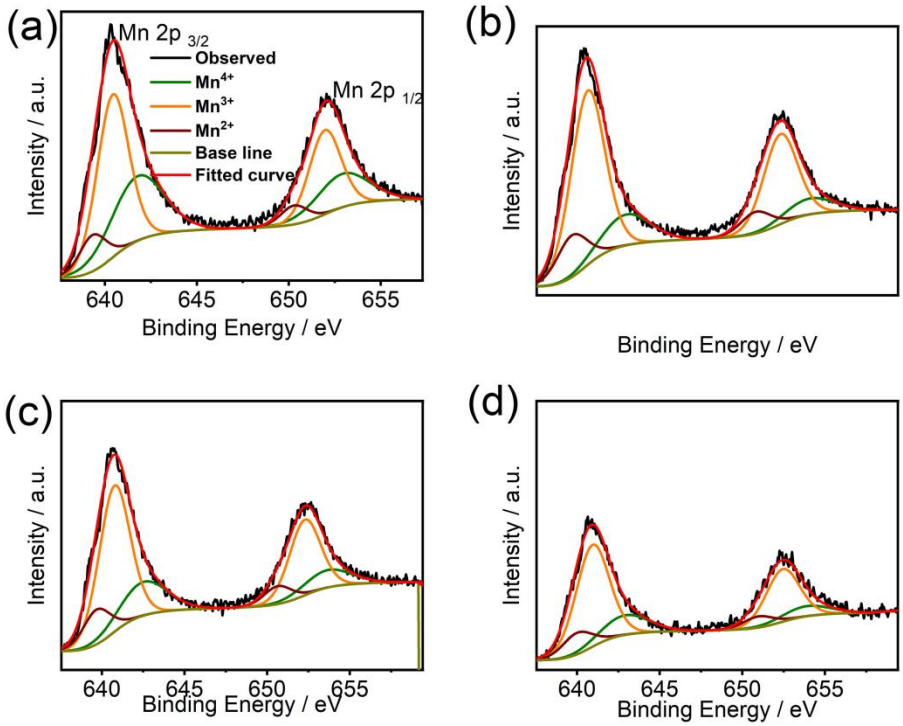

Fig. S 3 XPS spectra (black) and the fitted curves (red) of the FeMO (a), 0.35%InFeMO (b), 0.7%InFeMO (c) and 1.4%InFeMO (d). Brown, orange and green curves are the contribution from the Mn 2p orbitals of Mn^{2+}, Mn^{3+} and Mn^{4+}.

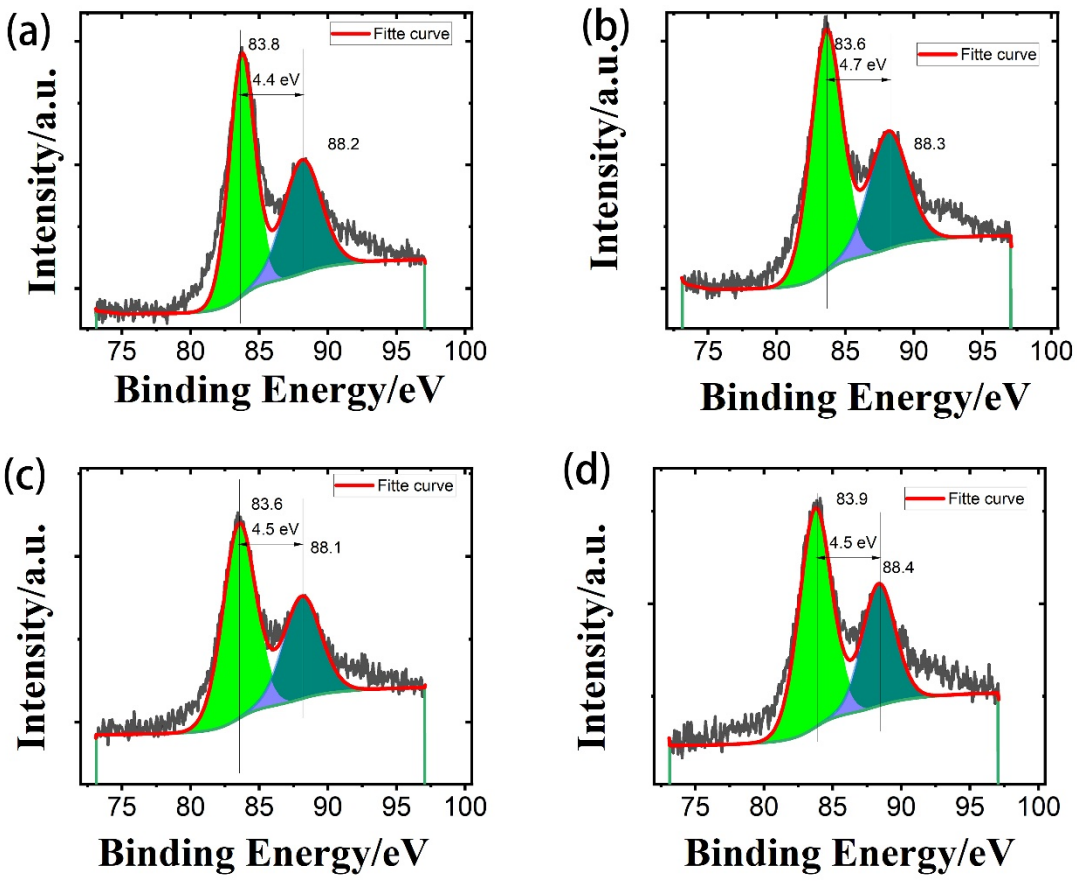

Fig. S 4 XPS spectra (black) and the fitted curves (red) of the Mn 3s orbital of FeMO (a), 0.35%InFeMO (b), 0.7%InFeMO (c) and 1.4%InFeMO (d).

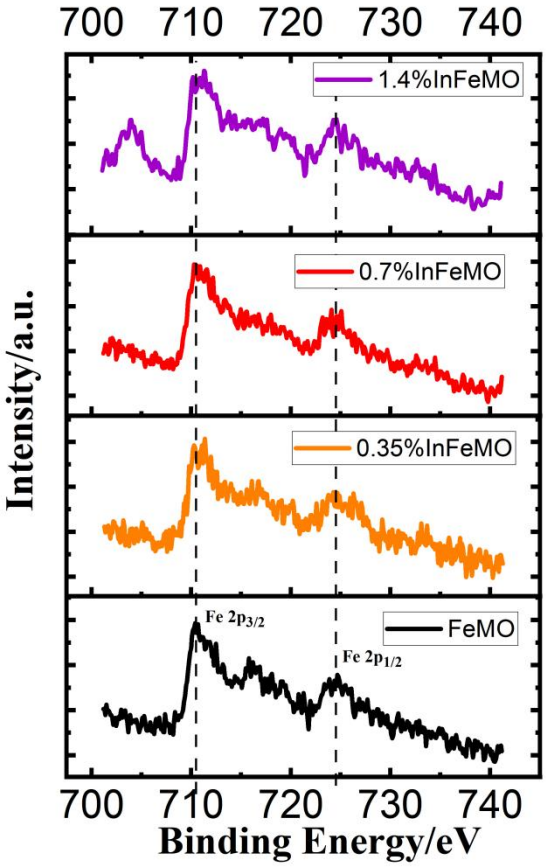

Fig. S 5 XPS spectra of Fe 2p obtained from the FeMO, 0.35%InFeMO, 0.7%InFeMO and 1.4%InFeMO.

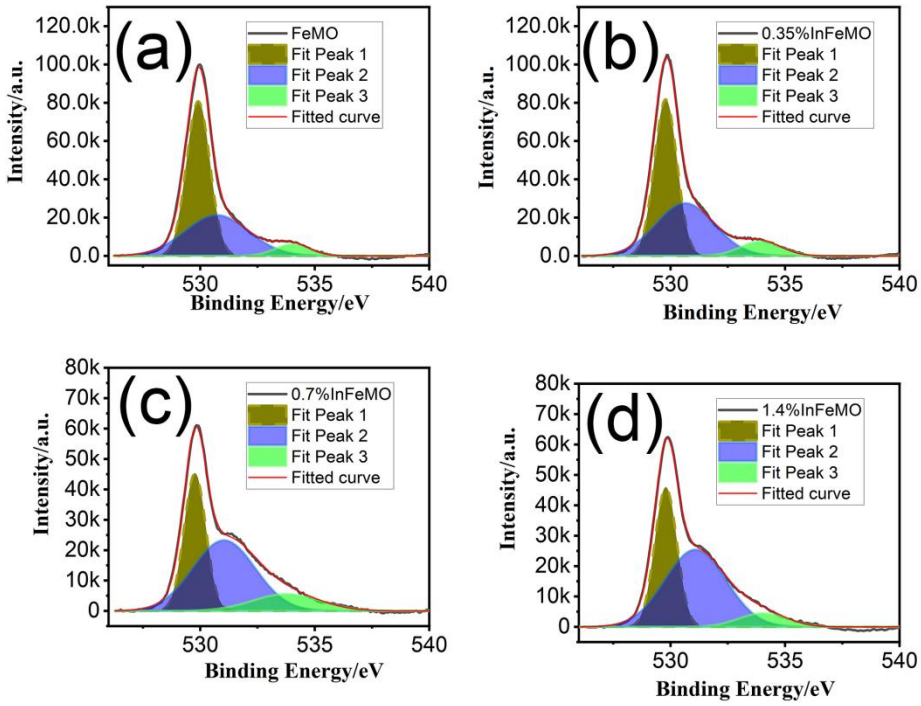

Fig. S 6 XPS spectra of O 1s obtained from the FeMO, 0.35%InFeMO, 0.7%InFeMO and 1.4%InFeMO.

Table S 1 Areal Ratio of the fit peaks of different oxygen species from XPS spectra of O 1s .

Peaks	Peak location /eV	Corresponding oxygen species	Areal Ratio / %			
			FeMO	0.35%InFeMO	0.7%InFeMO	1.4%InFeMO
1	529	lattice oxygen	54.8	49.2	35.1	36.5
2	531	adsorbed oxygen	39.2	42.7	51.6	55.8
3	533	hydroxyl oxygen	6.0	8.1	13.3	7.7

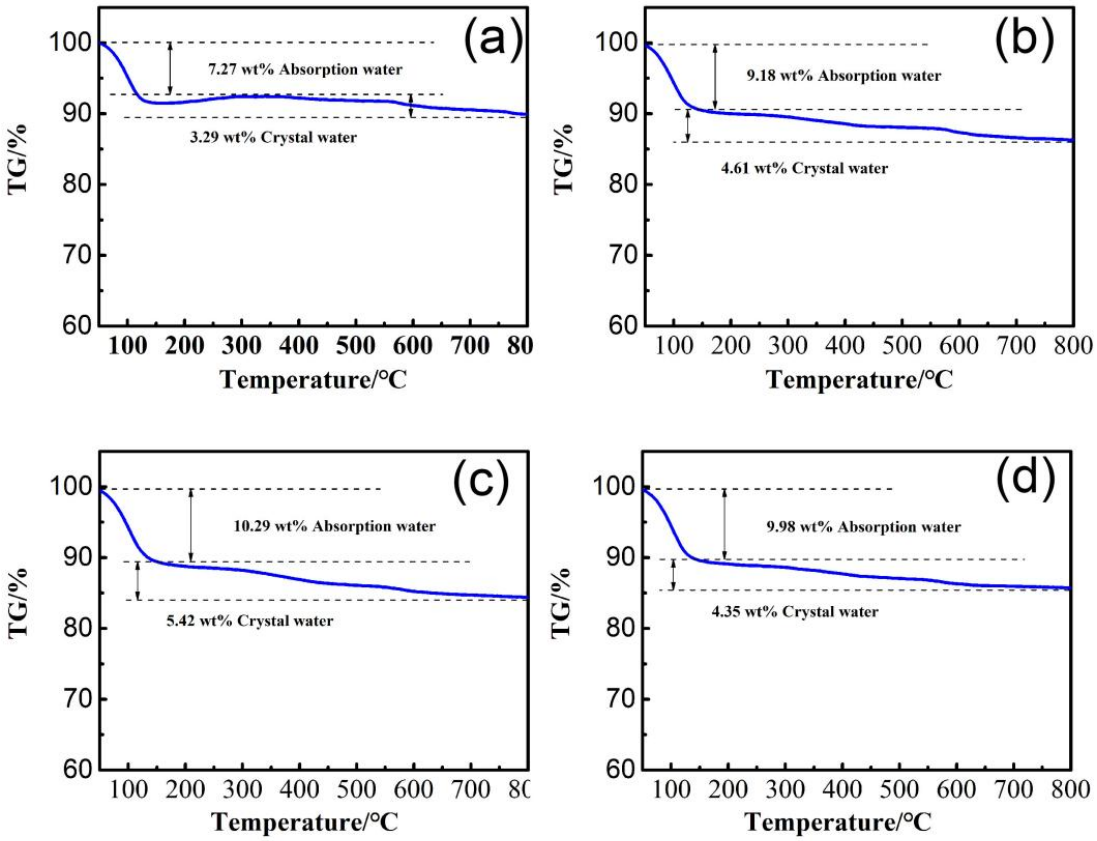

Fig. S 7 Thermogravimetric curves of the FeMO, 0.35%InFeMO, 0.5%InFeMO, 0.7%InFeMO and 1.4%InFeMO.

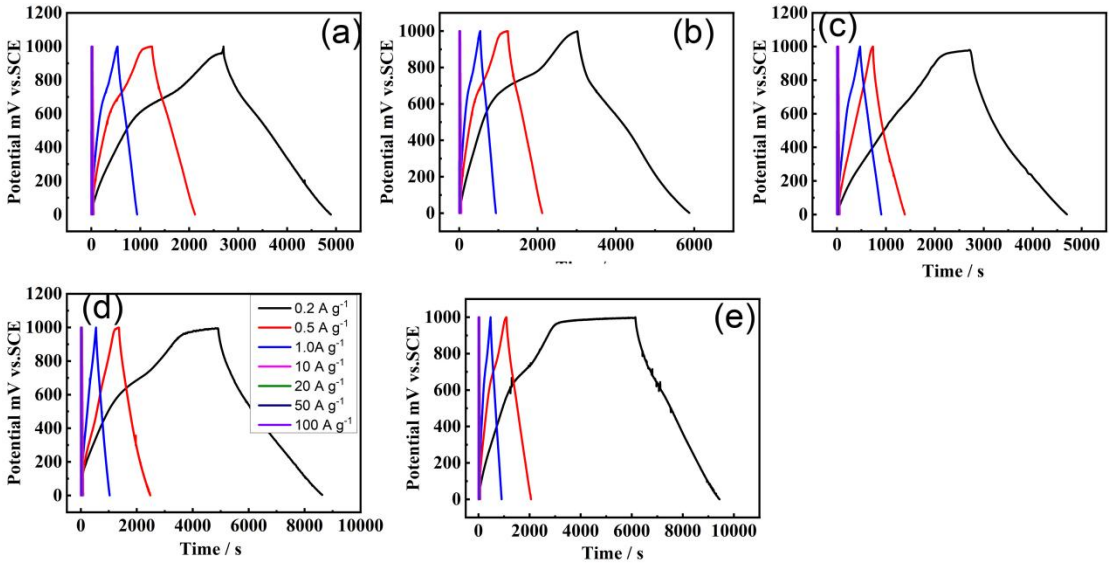

Fig. S 8 Charge/discharge curves of the PMO (a), FeMO (b), 0.35%InFeMO (c), 0.7%InFeMO (d) and 1.4%InFeMO (e) electrodes at different current density. They share the same legends with (d).

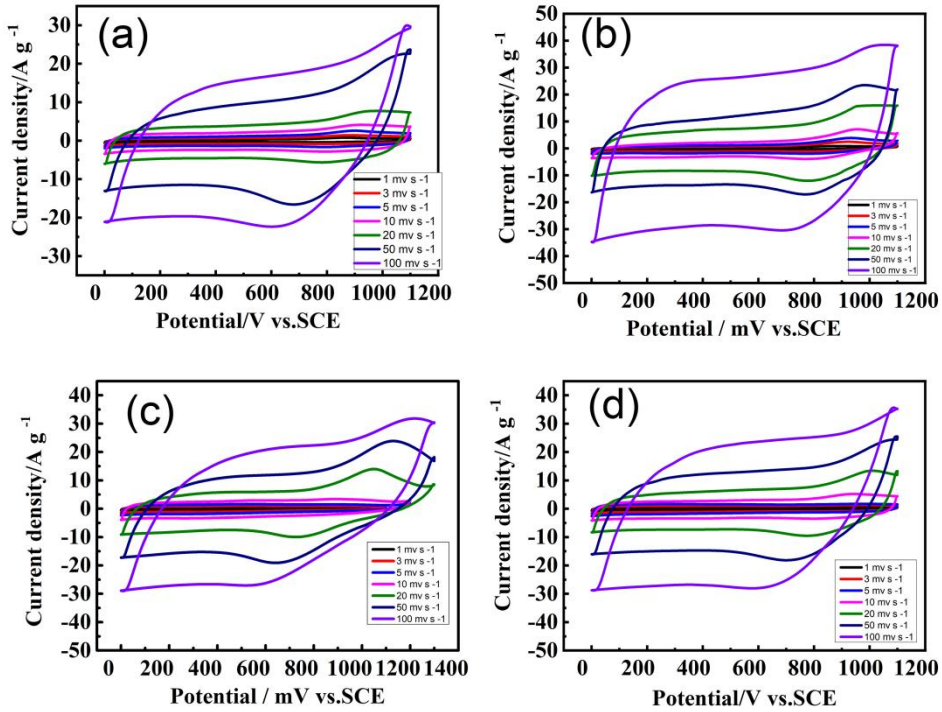

Fig. S 9 CV curves of the (a) PMO, (b) FeMO, (c) 0.35%InFeMO and (d) 1.4%InFeMO electrodes at various scan rate.

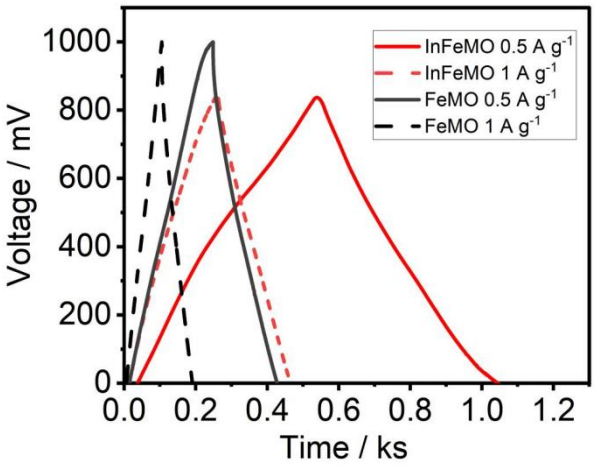

Fig. S 10 GCD curves of InFeMO and FeMO electrodes made from solution samples. Three electrodes are used for the measurement.

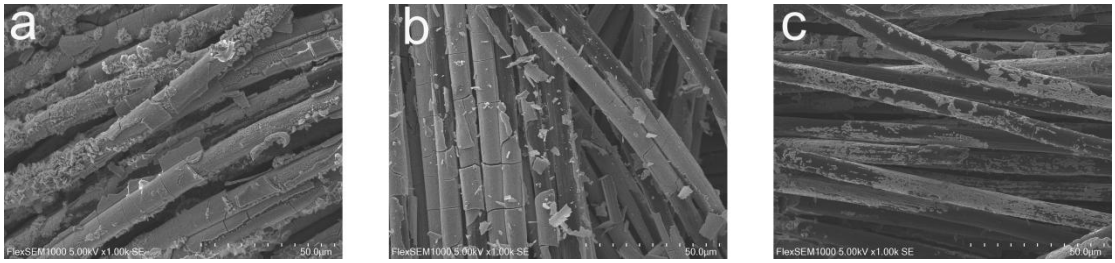

Fig. S 11 SEM images of cyclized carbon cloth covered by PMO, FeMO and 0.7%InFeMO, respectively.

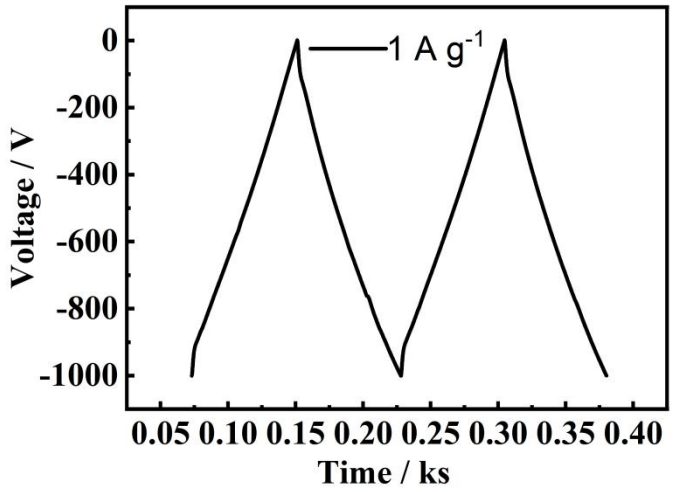

Fig. S 12 GCD curve of active carbon electrode at a mass loading of 35 mg cm^{-2}.

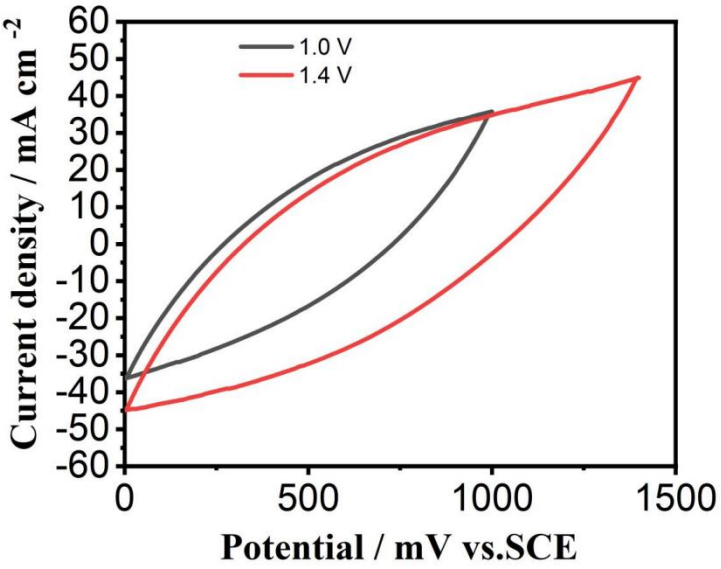

Fig. S 13 CV curves of the InFeMO electrode with high mass loading in different voltage windows at a scan rate of 20 mV s^{-1}.

Table S 2 Summary of Capacitive performance of the manganese oxide electrodes.

Substrates	Method	Mass Loading (mg cm^{-2})	Electrolyte	Gravimetric Capacitance (F g^{-1})	Areal Capacitance (mF cm^{-2})	Reference （DOI）
Carbon Cloth	Electrodeposition	0.15	1 M Na_2SO_4	1302	162 [1 A g^{-1}]	This work
Carbon Cloth	Electrodeposition	0.15	1 M Na_2SO_4	1302	195 [0.3 A g^{-1}]	This work
Carbon Cloth	Electrodeposition	10.6	1 M Na_2SO_4	180 [1 A g^{-1}]	1908 [1 A g^{-1}]/[10 mA cm^{-2}]	This work
Carbon Cloth	Electrodeposition	10.6	1 M Na_2SO_4	182 (0.3 A g^{-1})	1929 [0.3 A g^{-1}]	This work
Carbon Cloth	Electrodeposition	9.14	1 M Na_2SO_4	160 [1A cm^{-2}]	1570 [1A cm^{-2}]	10.1039/d1ta04850c
Carbon Cloth	Electrodeposition	7.5	5 M LiCl	173.3	1300 [5 mV s^{-1}]	10.1021/acsenergylett.7b00405
Carbon Cloth	Electrodeposition	10.0	1 M Na_2SO_4	304 [3 mA cm^{-2}]	3040 [3 mA cm^{-2}]	10.1021/acsnano.8b00621

Substrates	Method	Mass Loading (mg cm^{-2})	Electrolyte	Gravimetric Capacitance (F g^{-1})	Areal Capacitance (mF cm^{-2})	Reference （DOI）
Carbon Cloth	Redox deposition with $KMnO_4$	3.4	1 M LiCl	152	517	10.1039/c6mh00556j
Carbon Cloth	Electrodeposition	3.7	5 M LiCl	243 [1 mA cm^{-2}]	900	10.1016/j.jpowsour.2018.06.026
Carbon Cloth	Electrodeposition	7.0	5 M LiCl	234 [1 mA cm^{-2}]	1638 [1 mA cm^{-2}]	10.1016/j.jpowsour.2018.06.026
Carbon Fiber	Electrodeposition	3.1	1 M Na_2SO_4	170 [3 mA cm^{-2}]	526	10.1016/j.jpowsour.2018.06.026
Carbon Cloth	Redox deposition with $KMnO_4$	2	1M Na_2SO_4	366	732	10.1016/j.cej.2021.128967
Carbon cloth	Redox deposition with $KMnO_4$	3.37	1 M LiCl	178 [0.3 A g^{-1}]	783 [0.3 A g^{-1}]	10.1039/C6MH00556J
Stainless steel	Ultrasonic reaction with rGO and MWCNT	12.0	1 M Na_2SO_4	314.6 [5 mV s^{-1}]		10.1016/j.ultsonch.2021.105896
Special Substrates						
Mesoporous Au	Redox deposition with $KMnO_4$	-	1 M Na_2SO_4	906.4	-	10.1007/s13404-017-0196-x
Nanoporous Au	Electrodeposition	-	2 M Li_2SO_4	1145	-	10.1038/NNANO.2011.13
Graphite foil	Electrodeposition	0.23	3 M KCl	1061	244	10.1039/C4NR06559J
carbon nanotube	Electrodeposition	-	1M Na_2SO_4	1230	-	10.1021/nl2023433
Ni dendrites	Electrodeposition	0.35	1M Na_2SO_4	1125	394	10.1039/c3nr00209h
Porous carbon cloth	Redox deposition with $KMnO_4$	4.5	5 M LiCl	464	2088	10.1016/j.ensm.2017.05.007
Carbon Fiber	Electrodeposition	3.8	0.5 M Na_2SO_4	~70	~266	10.1021/nn203085j

Substrates	Method	Mass Loading (mg cm^{-2})	Electrolyte	Gravimetric Capacitance (F g^{-1})	Areal Capacitance (mF cm^{-2})	Reference （DOI）
Carbon Fiber	Electrodeposition	8.3	0.5 M Na_2SO_4	337 [0.05 mV s^{-1}]	2800 [0.05 mV s^{-1}]	10.1021/nn203085j